Developmentally distinct CD4$^+$ T$_{reg}$ lineages shape the CD8$^+$ T cell response to acute *Listeria* infection

Joseph S. Dolina[a] , Joey Lee[a], Eugene L. Moore[b], Jennifer L. Hope[c], Donald T. Gracias[d], Takaji Matsutani[e] , Ashu Chawla[f], Jason A. Greenbaum[f] , Joel Linden[a] , and Stephen P. Schoenberger[a,1]

[a]Division of Developmental Immunology, La Jolla Institute for Immunology, La Jolla, CA 92037; [b]Division of Vaccine Discovery, La Jolla Institute for Immunology, La Jolla, CA 92037; [c]Tumor Microenvironment and Cancer Immunology Program, Sanford Burnham Prebys Medical Discovery Institute, La Jolla, CA 92037; [d]Division of Immune Regulation, La Jolla Institute for Immunology, La Jolla, CA 92037; [e]Research and Development Department, Repertoire Genesis Incorporation, 567-0085 Ibaraki, Osaka, Japan; and [f]Bioinformatics Core, La Jolla Institute for Immunology, La Jolla, CA 92037

CD4$^+$ regulatory T cells (T$_{regs}$) must prevent immunopathology by cytotoxic CD8$^+$ T lymphocytes (CTLs) responding to acute infection and restore immune homeostasis following pathogen clearance, yet little is known about the specific populations or mechanisms governing these discrete events. We found that acute *Listeria monocytogenes* (*L. monocytogenes*) infection produces a phenotypically and functionally complex T$_{reg}$ response comprising two separate suppressor cell subpopulations, with an early T$_{reg}$ peak occurring at 24 h postinfection and a later peak arising by day 7. The first wave of T$_{regs}$ suppress primary CTL expansion via a contact-independent mechanism involving CD73-derived adenosine (Ado) production from extracellular adenosine monophosphate (5′-AMP), while the second originates from different precursors and acts throughout the contraction phase via contact-dependent gap junction transfer of 3′,5′-cyclic adenosine monophosphate (cAMP)—both potent inhibitors of T cell proliferation. We speculate that the early activation of CD73 on T$_{regs}$ is enhanced in inflamed tissues due to high purine release from apoptotic cells, whereas late-phase gap junction–dependent T$_{regs}$ rely more on cell number and less on tissue inflammation. This study importantly reveals that CTL priming and contraction phases are separately fine-tuned by developmentally distinct T$_{reg}$ lineages during an acute infection.

FoxP3$^+$ T regulatory cell | CD73 | gap junction | cyclic AMP | *Listeria monocytogenes*

T$_{regs}$ comprise a heterogeneous T cell population within the CD4$^+$ compartment based on their organ/tissue niche occupancy, T cell receptor (TCR) repertoire, transcription factor profile, surface marker display, and mechanism of suppression (1–3). Natural CD4$^+$ regulatory T cells (nT$_{regs}$) develop in the thymus, coexpress the α-chain of the high-affinity IL-2 receptor (CD25) and the X-linked transcription factor forkhead box P3 (FoxP3), and are required for the maintenance of immune tolerance to self-antigens during homeostasis (4). Functional loss of *Foxp3* has been shown to underlie a range of lymphoproliferative and autoimmune disorders in both mice and humans (5–8). FoxP3 expression can also be induced in conventional FoxP3$^−$CD4$^+$ T cells (T$_{convs}$) under inflammatory or noninflammatory conditions, resulting in the generation of a second type of T$_{reg}$ called peripheral CD4$^+$ regulatory T cells (pT$_{regs}$) (9, 10).

In addition to a documented role in controlling self-reactivity, T$_{regs}$ can also influence the magnitude and severity of acute and chronic infections through suppression of pathogen-specific T$_{convs}$ and CTLs (11, 12). Accordingly, clearance of microbial pathogens is promoted by depletion of nT$_{reg}$ and pT$_{reg}$ populations and/or inhibition of single suppressor pathways, albeit with an increased risk of autoimmune side effects (13). The specific effector mechanisms underlying T$_{reg}$-mediated control in such cases appear to vary with different infections and distinct phases of the immune response. For example, IL-2 deprivation can alone inhibit CD4$^+$ and CD8$^+$ T cell responses during autoimmunity and *Toxoplasma gondii*, *L. monocytogenes*, and vaccinia virus infections (14, 15). During hepatitis C virus (HCV) infection, T$_{reg}$ suppression has been shown to be mainly dependent on TGF-β production and cell contact (16, 17). Other pathways are more controversial and context specific. IL-10 has been shown to contribute to T$_{reg}$-mediated suppression of CD8$^+$ T cells during *L. monocytogenes* infection of pregnant hosts (18). However, throughout acute lymphocytic choriomeningitis virus (LCMV Armstrong) infection, FoxP3$^+$ T$_{reg}$-derived IL-10 was shown conversely to "insulate" CD8$^+$ T cells from proinflammatory signals in the primary response, indirectly promoting memory differentiation of these cells (19). There also appears to be both quantitative and temporal control of T$_{regs}$ in acute *L. monocytogenes* infection, as the degree to which they inhibit protective CTLs depends on the initial infectious dose and associated early inflammatory cues (20), where the developing infection eventually overrides early baseline T$_{reg}$ function to allow for the rapid clonal expansion of CTLs 72 h after *L. monocytogenes* exposure (14, 21). There are currently significant gaps in our understanding of the quantitative and functional features of T$_{reg}$ development during priming/expansion versus contraction phases of an acute infection, although such information could meaningfully

Significance

The CD4$^+$ T$_{reg}$ response following acute *Listeria* infection is heterogeneous and deploys two distinct modes of suppression coinciding with initial pathogen exposure and resolution of infection. This bimodal suppression of CD8$^+$ T cells during priming and contraction is mediated by separate T$_{reg}$ lineages. These findings make a significant contribution to our understanding of the functional plasticity inherent within T$_{regs}$, which allows these cells to serve as a sensitive and dynamic cellular rheostat for the immune system to prevent autoimmune pathology in the face of inflammation attendant to acute infection, enable expansion of the pathogen-specific response needed to control the infection, and reestablish immune homeostasis after the threat has been contained.

inform our understanding of immune protection versus pathology in this setting.

Prior studies suggest that the T_{reg} response to acute infection may involve distinct, and perhaps contextual, phases of immunoregulatory function. We hypothesize that, in contrast to the stable population dynamics associated with chronic viral infection, the priming, expansion, and contraction of T_{regs}, T_{convs}, and CTLs are coordinately regulated throughout the primary response to acute infection to prevent immune pathology and facilitate pathogen control. In this study, we have applied a variety of phenotypic, genetic, and functional tools to follow the dynamic evolution of the T_{reg} response during acute *L. monocytogenes* infection and monitor its effect on pathogen-specific CTLs. Our results demonstrate that the $CD8^+$ T cell response is regulated by developmentally distinct T_{reg} populations that employ different suppressor mechanisms across different phases of the immune response against a single acute infection.

Results

Functional and Phenotypic Evolution of the T_{reg} Response to Acute *Listeria* Infection. Intravenous (IV) infection of C57BL/6 hosts with *L. monocytogenes* Δ*actA*-Ova (an attenuated *L. monocytogenes* strain deleted for the actin assembly–inducing protein and expressing chicken ovalbumin) produces a distinct T_{reg} response in terms of magnitude and kinetics, depending on the initial inoculum size (20). Acute infection with 1×10^6 colony-forming units (CFU) causes a rapid rise in the absolute number of T_{regs} measured at 24 h and the subsequent appearance of a second T_{reg} peak at day 7 (Fig. 1*A*) (20). To evaluate the relative suppressive capacity of day 1 versus day 7 T_{regs}, we used a FoxP3-eGFP reporter system that allows for isolation of T_{regs} (22). $CD4^+FoxP3$-$eGFP^+$ T_{regs} were isolated at 1, 3, or 7 d following infection of *Foxp3^eGFP* mice and tested for their ability to inhibit CD3/CD28-mediated proliferation of polyclonal $CD45.1^+CD8^+$ responder T cells (T_{resps}). The in vitro suppressive capacity of nT_{regs} isolated from naïve *Foxp3^eGFP* mice was comparable on a per-cell basis to T_{regs} isolated from mice 1 d postinfection (day 1 T_{reg}) with ~50% $CD8^+$ T_{resp} suppression in

1:1 T_{reg}:T_{resp} cocultures (Fig. 1 *B* and *C*). This cell-intrinsic suppressor activity was rapidly lost in T_{regs} isolated at day 3 postinfection compared to nT_{regs} and day 1 T_{regs} paralleling the drop in total T_{reg} absolute number (Fig. 1 *A–C*). Suppressor activity was again evident in T_{regs} isolated at day 7 postinfection (day 7 T_{reg}), which displayed a significantly greater suppressive capacity per cell than that of T_{regs} isolated at earlier time points (days 0 to 1) (Fig. 1 *B* and *C*). These findings demonstrate that T_{reg} activity varies over time during acute *L. monocytogenes* infection in that it is present at day 1 (priming phase) and at day 7 (contraction phase) but is notably absent during the period coincident with effector $CD8^+$ T cell expansion (days 3 to 6).

We next sought to investigate lineage relationships between the early (day 1) and later (day 7) T_{reg} populations. We first performed differential kinetic labeling studies by intraperitoneally (IP) administering 5-ethynyl-2'-deoxyuridine (EdU) to *Foxp3^eGFP* mice at the time of infection to allow tagging of day 1 T_{regs} followed by IP delivery of 5-bromo-2'-deoxyuridine (BrdU) at day 5 postinfection, just prior to the emergence of day 7 T_{regs} (*SI Appendix*, Fig. S1*A*). Examination of the $CD4^+FoxP3$-$eGFP^-$ T_{conv} and $CD4^+FoxP3$-$eGFP^+$ T_{reg} subsets showed that the majority of labeled populations were single positive for either EdU or BrdU, suggesting that proliferating $CD4^+$ T cells present at either day 1 or day 7 largely arise through proliferation of different precursors (*SI Appendix*, Fig. S1 *B* and *C*). Minor populations (0.1 to 0.2%) of $CD4^+$ T cells were consistently detected within T_{conv} (both EdU^{lo} and EdU^{hi}) and T_{reg} (EdU^{hi}) compartments that costained for BrdU (*SI Appendix*, Fig. S1 *B* and *C*), indicating that a small percentage of T_{regs} at day 7 could derive from day 1 T_{regs}. Despite appearing that day 1 T_{regs} decline in absolute number shortly after infection (Fig. 1*A*), it is also possible that early T_{regs} undergo extensive division, becoming entirely negative for EdU.

To further establish that day 1 and day 7 T_{regs} represent distinct populations, we compared the TCR repertoires of T_{conv} and T_{reg} populations obtained via hemisplenectomy at these two time points within individual animals undergoing infection, thus allowing serial sampling of a given spleen. $CD4^+FoxP3$-$eGFP^-$ T_{convs} and $CD4^+FoxP3$-$eGFP^+$ T_{regs} were sorted at each
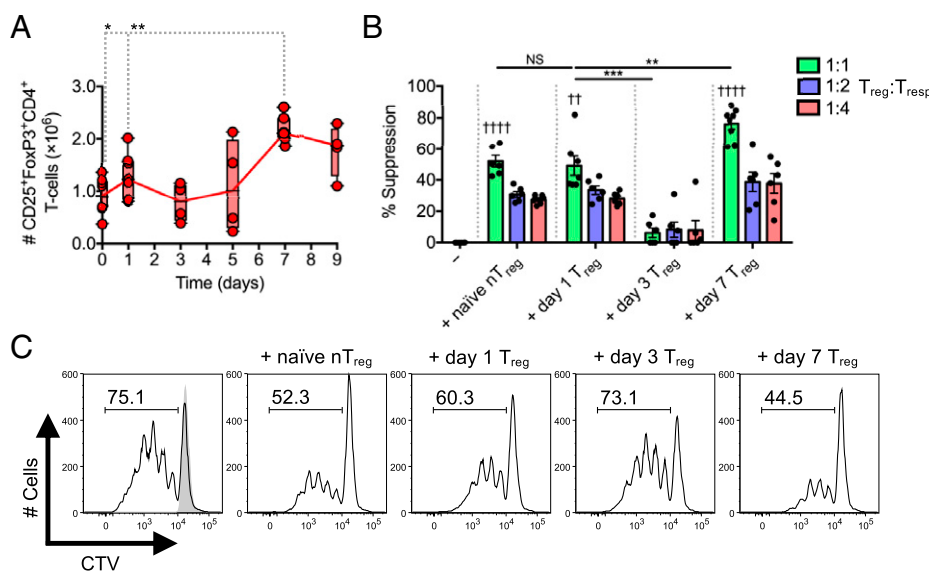

Fig. 1. T_{reg} responses during *Listeria* infection display a biphasic kinetic pattern. C57BL/6 mice infected with *L. monocytogenes* Δ*actA*-Ova. (*A*) Number of $CD25^+FoxP3^+CD4^+$ T_{regs} in spleens 0 to 9 d postinfection ($n = 4$ to 8 per group). (*B* and *C*) In vitro $CD45.1^+CD8^+$ T_{resps} proliferation/percent suppression at day 3 after coculture with $CD45.2^+CD4^+FoxP3$-$eGFP^+$ T_{regs} isolated from naïve *Foxp3^eGFP* mice and those that underwent 1, 3, or 7 d of infection. Indicated are titrated T_{reg}:T_{resp} ratios after anti-CD3/CD28 stimulation ($n = 4$ per group). Reported in histograms are percentage and data from 1:1 T_{reg}:T_{resp} cocultures. Mean ± SEM; (*A* and *B*) *$P < 0.05$, **$P < 0.01$, and ***$P < 0.001$ (Student's t test); (*B*) ††$P < 0.01$ and ††††$P < 0.0001$ (one-way ANOVA relative to $-T_{reg}$). CTV, CellTrace Violet; NS, not significant.

Dolina et al.
Developmentally distinct $CD4^+$ T_{reg} lineages shape the $CD8^+$
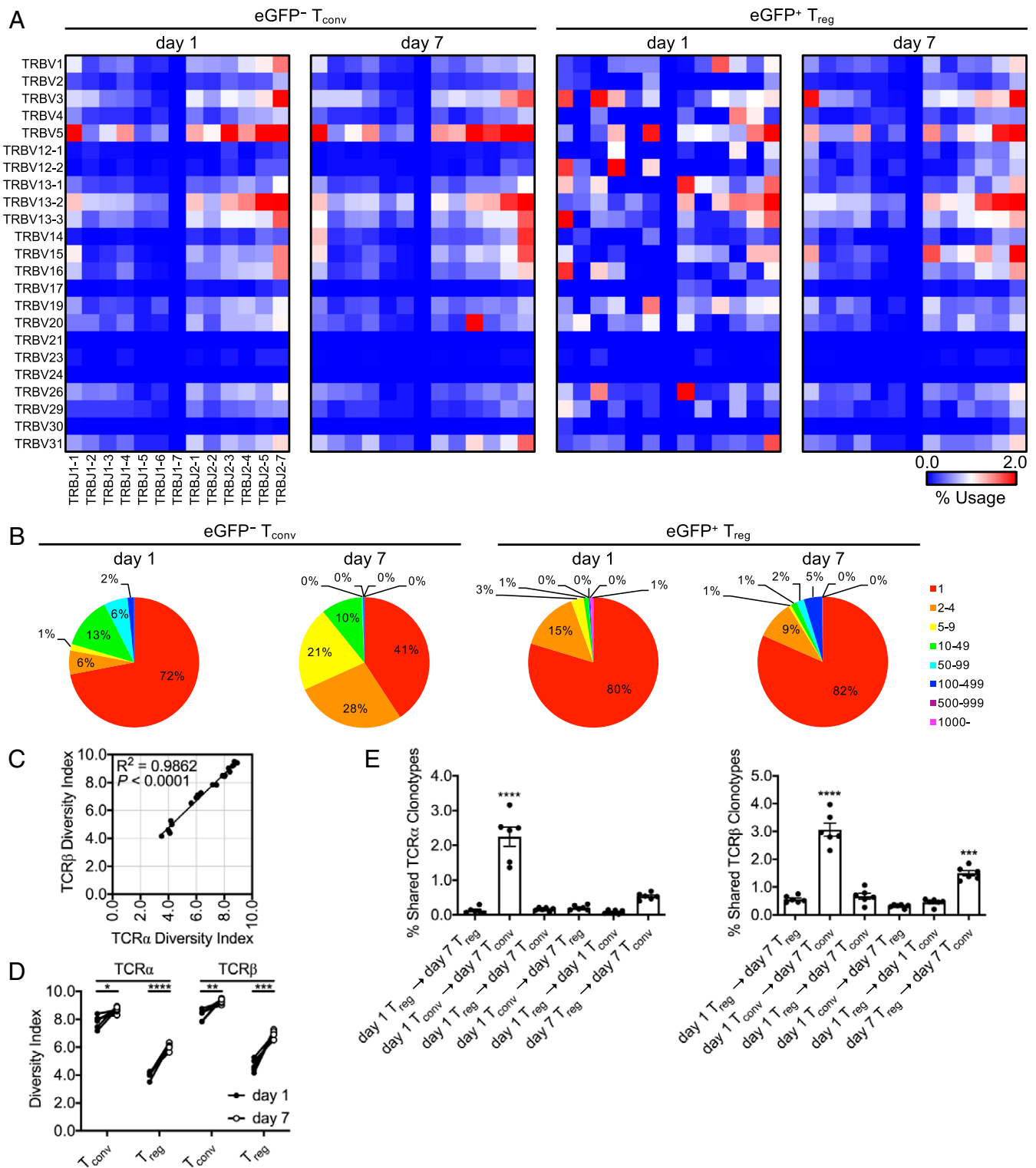T cell response to acute *Listeria* infection

Fig. 2. Splenic T_{regs} do not display clonal expansion during *Listeria* infection. *Foxp3*^{eGFP} mice infected with *L. monocytogenes* Δ*actA*-Ova. Hemisplenectomy was performed at day 1 postinfection, and viable NK1.1⁻CD4⁺TCR-β⁺FoxP3-eGFP⁻ (T_{conv}) and FoxP3-eGFP⁺ (T_{reg}) cell populations were cell sorted from the dorsocranial lobe of the spleen. Corresponding cell populations were isolated at day 7 from the remaining ventral-caudal half of the spleen. Total RNA was isolated from all cells and subjected to TCR-Seq. (*A*) TCRβ *Trb* V (TRBV) and *Trb* J (TRBJ) gene segment family average usage among animals. (*B*) Representative number of *Trb* CDR3 clone reads. (*C* and *D*) Shannon–Weaver TCR diversity indices reported. (*E*) Intraanimal Venn analysis displaying shared *Tra* and *Trb* CDR3 clonotypes (n = 6 per group, 3 male and 3 female). Mean ± SEM. (*C*) R^2/*P* (linear regression analysis); (*D*) **P* < 0.05, ***P* < 0.01, ****P* < 0.001, and *****P* < 0.0001 (Student's *t* test); and (*E*) ****P* < 0.001 and *****P* < 0.0001 (one-way ANOVA).

Dolina et al.
Developmentally distinct CD4⁺ T_{reg} lineages shape the CD8⁺
T cell response to acute *Listeria* infection

PNAS | 3 of 12
https://doi.org/10.1073/pnas.2113329119

time point, and TCR sequencing (TCR-Seq) was performed to determine the repertoire of V and J gene segments expressed by TCRα (*Tra*) and TCRβ (*Trb*) gene loci in each subset. In cells isolated at day 1 postinfection, interanimal average V and J gene segment family usage at the *Tra* (*SI Appendix*, Fig. S2) and *Trb* (Fig. 2*A*) loci were randomly distributed in both T_{convs} and T_{regs}. By day 7, however, the usage of particular segment combinations increased. In day 7 T_{convs}, we observed predominant usage of TRAV4D-4/TRAJ48, TRBV20/TRBJ2-3, and TRBV14/TRBJ2-7 that was not apparent in day 1 T_{convs} and overall increased expression of combinations within TRBV5. Moreover, the pattern of gene segment family usage between T_{convs} and T_{regs}, though distinct at day 1, more closely resembled each other by day 7 (Fig. 2*A* and *SI Appendix*, Fig. S2 and Table S1). As infection progressed, the number of clonal *Trb* CDR3 reads in both T_{conv} and T_{reg} subsets increased in frequency from day 1 to day 7; however, T_{convs} appeared to undergo more clonal expansion compared to T_{regs}. More repetitive CDR3 reads were apparent in T_{regs} at day 7, also suggesting that T_{regs} develop into larger, but fewer, clones compared to T_{convs} (Fig. 2*B*). This was also consistent with increased overall TCR diversity in T_{convs} that changed less over time versus observations in T_{regs} (Fig. 2 *C* and *D*). These results suggest that T_{conv} and T_{reg} responses shift from a polyclonal to an oligoclonal repertoire at different rates and/or selectivities.

Finally, we compared *Tra* and *Trb* CDR3 sequences shared between T_{convs} and T_{regs} via intraanimal Venn analysis at day 1 and day 7. As expected, a strong clonal relationship existed between day 1 and day 7 T_{conv} subsets (as both shared TCRα and TCRβ clonotypes), supporting the notion that expansion of antigen-specific effector CD4$^+$ T cells had occurred. Importantly, we did not observe any clonal similarity between day 1 and day 7 T_{reg} populations, reinforcing our prior conclusion that these biphasic T_{reg} populations are developmentally unrelated, yet retain the capacity to differentially suppress CTLs at distinct stages of the primary response to *L. monocytogenes* (Fig. 2*E*). Regardless of the origin of T_{regs}, our data clearly demonstrate that day 7 T_{regs} are not simply derived from increased expansion of the original T_{reg} population present at day 1.

Early and Late T_{reg} Development Is Linked to Specific Gene Expression Signatures. Having established that day 1 and day 7 T_{regs} were distinct in their ontogeny and TCR repertoire, we surveyed the suppressor mechanisms associated with these cells. To accomplish this, *Foxp3*^{eGFP} mice were infected, and CD4$^+$FoxP3-eGFP$^+$ T_{regs} were isolated at days 0, 1, 3, and 7 for RNA sequencing (RNA-Seq). Unbiased hierarchical clustering of T_{reg}-linked suppressor function genes identified highly dynamic and temporally regulated gene sets with the strongest expression of T_{reg}-associated genes observed at days 0, 1, and 7. With the notable exception of *Ctla4* (CTLA-4) and *Il10* (IL-10), most T_{reg}-associated genes were transcriptionally inactive at day 3, consistent with lack of functional suppression observed at this time point (Fig. 1 *B* and *C* and 3*A*). Gene set enrichment analysis (GSEA) of gene clusters 1 to 3 (C1-3) revealed that C2, highly expressed before infection, was largely down-regulated from days 1 to 3 postinfection only to be partially up-regulated as part of the subsequent day 7 signature. A similar pattern of gene up-regulation shared between C2 (day 0 nT_{reg}) and C1 (day 7 T_{reg}) suggested that late-arising day 7 T_{regs} reacquire some original "nT_{reg}-like" transcripts but also induce transcription of new immunoregulatory genes at the contraction phase. In contrast, day 1 T_{regs} contained in the C3 gene cluster displayed a considerably enriched gene set (Fig. 3 *A* and *B*) that also segregated from all other time points using principal component analysis (PCA) (Fig. 3*C*).

Major suppressor genes, including *Ctla4*, *Tgfb1*, *Tgfb2*, and *Tgfb3* (TGF-β1/2/3), did not display a significant fold change in normalized expression between days 1 and 7. Day 1 T_{regs} had increased transcription of *Lgals9* (Gal-9), *Cd274* (PD-L1), *Tnfsf10* (TRAIL), *Gzmb* (granzyme B), *Lag3* (Lag-3), *Il10*, *Nt5e* (CD73), and *Gzma* (granzyme A), suggesting that these mechanisms may be relevant early after infection. In contrast, day 7 T_{regs} displayed increased expression of *Adcy3*, *Adcy7*, and *Adcy9* (adenylyl cyclases 3/7/9) and a significant decrease in *Pde4d* (phosphodiesterase 4) (Fig. 3*D*). This in turn suggested that late rising T_{regs} may accumulate intracellular cAMP (23, 24).

Pathway analysis confirmed a significant role for cAMP in day 7 T_{reg} function as several *Adcy*-linked pathways were up-regulated including peroxisome proliferator-activated receptor/retinoid X receptor (PPARα/RXRα) activation, eNOS signaling, α-adrenergic signaling, and cAMP-mediated signaling (Fig. 3*E*). In contrast, day 1 T_{regs} enriched for pathways related to innate immune signaling (interferon signaling and pattern recognition receptor [PRR] recognition of bacteria and viruses), apoptosis (death receptor signaling and retinoic acid–mediated apoptosis), abortive TCR signaling (protein kinase B [PI3K/AKT] and protein kinase A [PKA] signaling), and cell cycle inhibition (p53 signaling) consistent with its rapid induction but short lifespan (Fig. 3*E*). TGF-β1/2/3, despite not displaying a significant fold change in normalized expression between day 1 and day 7 T_{regs}, were not excluded in subsequent analyses because pathway analysis suggested TGF-β signaling and renin-angiotensin signaling (linked to TGF-β) were significantly up-regulated in day 7 T_{regs} (Fig. 3 *D* and *E*).

CD73 Expression Increases Early after Infection, while TGF-β Production and cAMP Accumulation Predominates during Contraction. We next determined whether the dynamic gene expression patterns revealed by RNA-Seq correlated with protein expression and were functionally relevant. T_{reg} CTLA-4 expression has been suggested to strip antigen presenting cells (APCs) of CD80/CD86; Lag-3 can bind major histocompatibility complex class II (MHC II) to modulate APC maturation and function; TRAIL, granzymes, and Gal-9 can induce apoptosis in T_{resps}; and IL-10 can exert antiinflammatory effects capable of negatively regulating T cell activation (1, 5, 25). Despite low levels of transcription at the *Ctla4* locus, both day 1 and 7 T_{regs} displayed equal amounts of CTLA-4 protein. In contrast, we could not detect TRAIL, Gal-9, Lag-3, and granzyme B protein in T_{regs} directly ex vivo. Trace IL-10 production was detected after phorbol 12-myristate 13-acetate (PMA)/ionomycin restimulation of T_{regs} at various time points (*SI Appendix*, Fig. S3*A*). Antibody blockade of TRAIL, Gal-9, Lag-3, and IL-10R in T_{reg}:T_{resp} cocultures did not reverse the suppression observed at either day 1 or day 7 (*SI Appendix*, Fig. S4*A*). Overall, these data indicate that most suppressor pathways differentially enriched in RNA-Seq and comparative GSEA related to direct T_{reg}:T_{resp} interaction did not yield a functional response to a known suppressor mechanism but rather likely reflect T_{reg} reactions to pro- and antiinflammatory cues at different time points.

T_{regs} express high levels of surface CD39 and CD73 ectonucleotidases, which dephosphorylate adenosine diphosphate/triphosphate (5'-ADP/5'-ATP) and 5'-AMP, respectively. Extracellular Ado produced by T_{reg} ectonucleotidase activity engages adenosine/A$_{2A}$ receptors (A$_{2A}$R) on CD8$^+$ T cells, whereas T_{reg} intracellular cAMP can be directly transferred to the cytosol of CD8$^+$ T cells via cell–cell contact. Both pathways separately lead to the inhibition of CTL proliferation, survival, and effector function due to the activation of PKA (23). T_{regs} can also use surface PD-L1 to suppress effector T cells by directly engaging the PD-1 inhibitory receptor (26). We evaluated protein expression of PD-L1, CD39, and CD73 as well as intracellular cAMP accumulation as genes associated with these suppressor
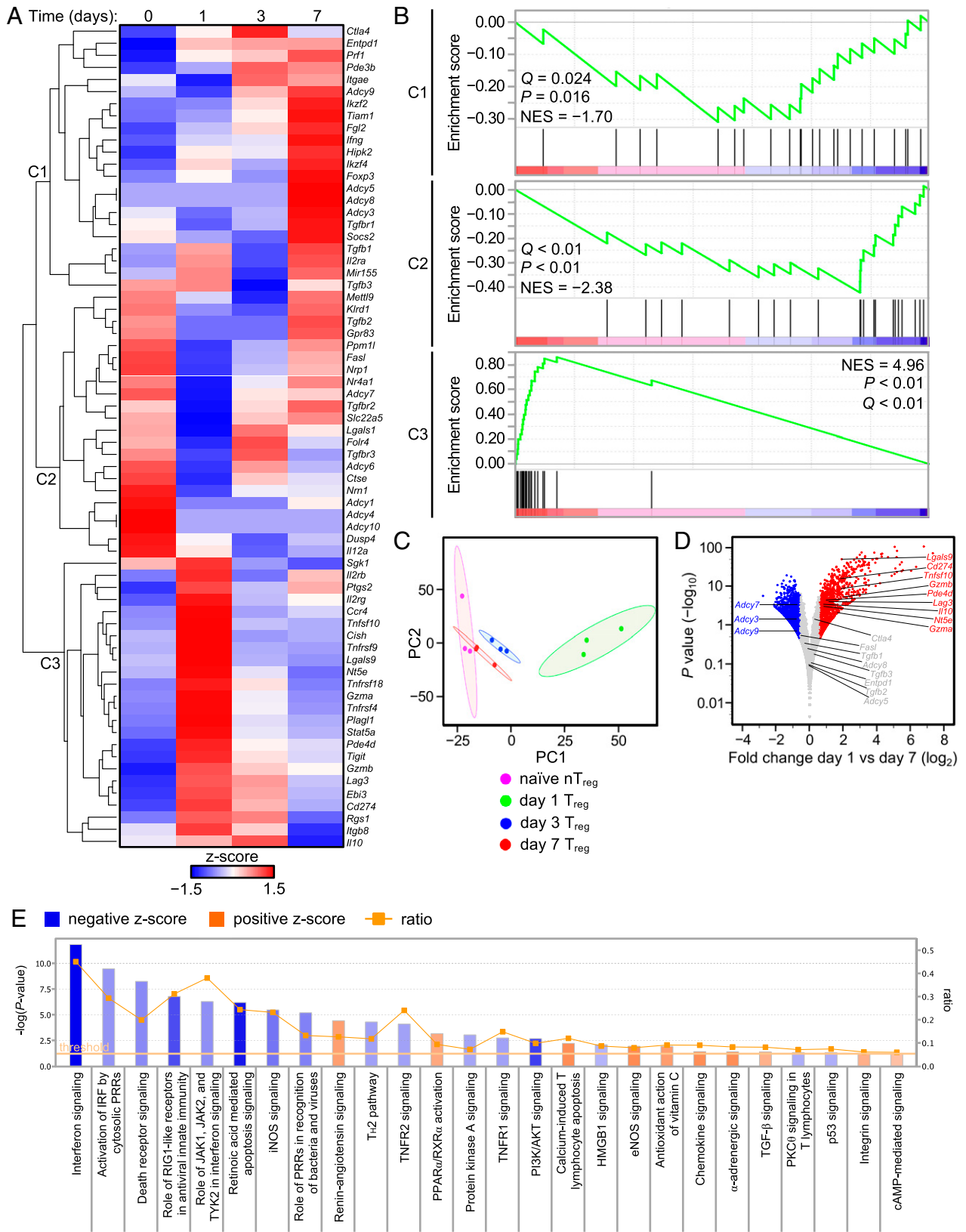
Fig. 3. Kinetic analysis of T_{reg} RNA-Seq. *Foxp3^eGFP* mice infected with *L. monocytogenes* Δ*actA*-Ova with total RNA isolated from NK1.1⁻CD4⁺TCR-β⁺FoxP3-eGFP⁺ T_{regs} at days 1, 3, and 7 postinfection or naïve animals. (*A*) RNA-Seq with hierarchical clustered, row-scaled log-transformed average reads per kilobase of transcript, per million mapped reads (RPKM) values. (*B*) GSEA against day 1 versus day 7 RNA-Seq comparisons performed with gene sets derived from clusters 1 to 3 (C1-3) in *A*. (*C*) PCA of T_{reg} RNA-Seq. (*D*) Volcano plot of selected genes and log₂ normalized expression with a Δ1.5 fold change cutoff against log₁₀ normalized *P* values from day 1 versus day 7 comparisons. (*E*) IPA canonical pathways associated with day 1 versus day 7 comparisons (*n* = 3 per group). Reported are lymphocyte-related pathways and ratio of pathway coverage (*P* < 0.05 threshold for gene network overlap).
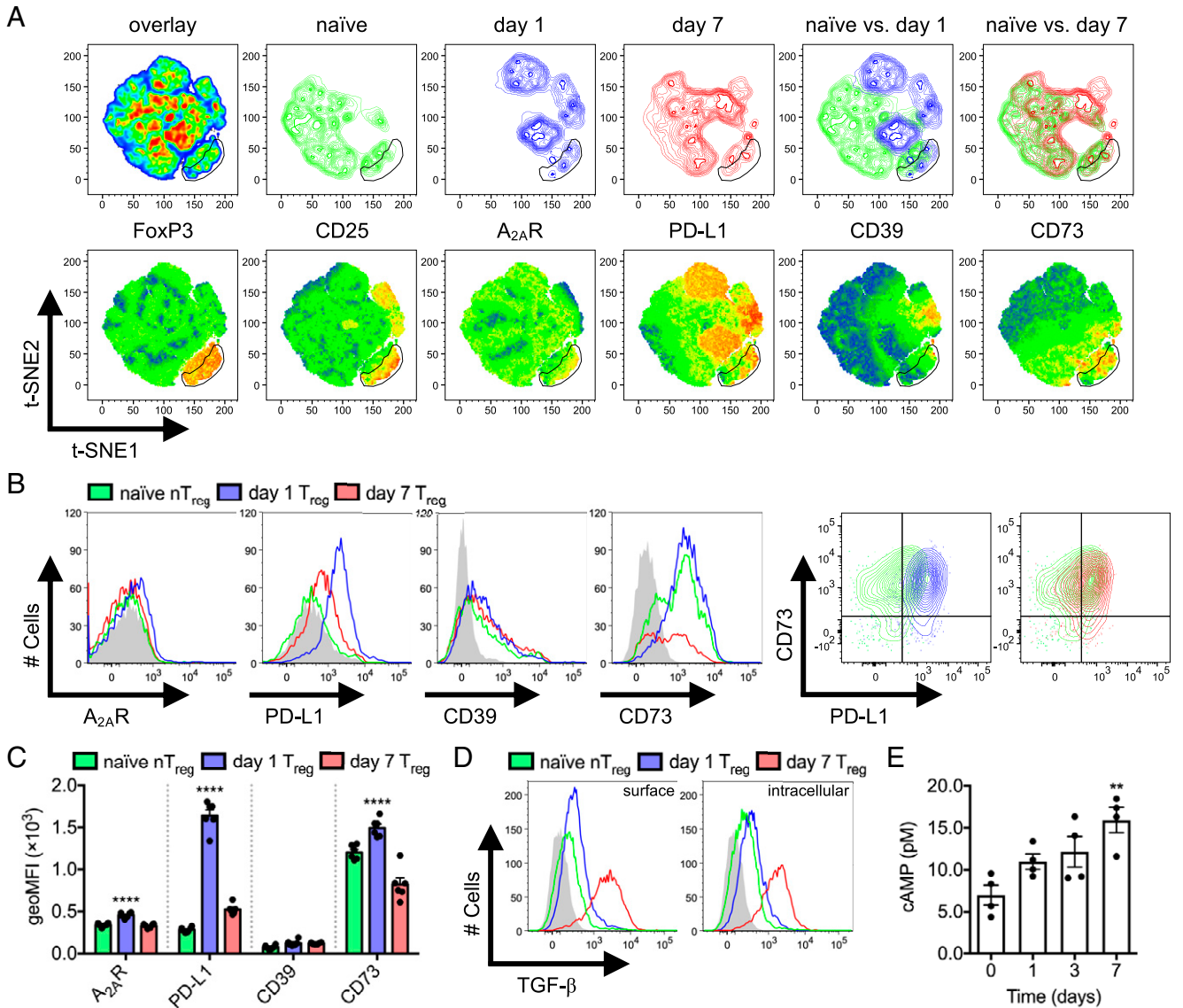
Dolina et al.
Developmentally distinct CD4⁺ T_{reg} lineages shape the CD8⁺
T cell response to acute *Listeria* infection

PNAS | 5 of 12
https://doi.org/10.1073/pnas.2113329119

Fig. 4. Temporal variation of T_{reg} effector mechanisms. Naïve compared to day 1 and 7 *L. monocytogenes* $\Delta actA$-Ova–infected C57BL/6 mice. (*A*) t-SNE analysis of CD4^{+} T cells with FoxP3, CD25, $A_{2A}R$, PD-L1, CD39, and CD73 dimensions. Density plots (*Upper*) and heatmap statistic displays of each input parameter (*Lower*) are displayed ($n = 6$ per group). (*B* and *C*) Expression of $A_{2A}R$, PD-L1, CD39, and CD73 on T_{reg} surface defined in *A* ($n = 6$ per group). (*D*) Expression of surface displayed and intracellular TGF-β by T_{regs} after PMA/ionomycin restimulation ($n = 4$ per group). (*E*) Intracellular FoxP3-eGFP[+] T_{reg} cAMP concentration after sorting from naïve *Foxp3*[eGFP] mice and those at days 1, 3, and 7 following *L. monocytogenes* $\Delta actA$-Ova infection ($n = 4$ per group). Filled histograms represent fluorescence minus one (FMO). Mean ± SEM. (*C* and *E*) **$P < 0.01$ and ****$P < 0.0001$ (one-way ANOVA).

pathways were differentially expressed in day 1 versus day 7 T_{regs}. The t-distributed stochastic neighbor embedding (t-SNE) clustering on total splenic CD4^{+} T cells isolated from naïve and day 1 versus day 7 infected mice was performed. Dimensional reduction using FoxP3, CD25, $A_{2A}R$, PD-L1, CD39, and CD73 was sufficient to segregate the day 1 T_{reg} clustering pattern from nT_{regs} and day 7 T_{regs} within a CD25^{+}FoxP3^{+}CD4^{+} T_{reg} gate on t-SNE plots (Fig. 4*A*). $A_{2A}R$, CD73, and PD-L1 expression peaked in day 1 T_{regs} to varying degrees, consistent with RNA-Seq findings (Fig. 4 *B* and *C*). Although PD-L1 expression peaked at day 1, this occurred on both FoxP3^{−} T_{convs} and FoxP3^{+} T_{regs} (Fig. 4*A*), and importantly, antibody blockade studies did not reveal a contribution to in vitro immunosuppression (*SI Appendix*, Fig. S4*A*). In contrast, maximal CD73 expression was observed within FoxP3^{+} T_{reg} populations. CD39 expression was apparent in only a small subset of FoxP3^{+} T_{regs}

and activated CD25^{lo}PD-L1^{+} T_{convs} (Fig. 4*A*), and its expression did not appear to vary throughout *L. monocytogenes* infection (Fig. 4 *B* and *C*). A separate t-SNE analysis of CD25^{+}FoxP3^{+}CD4^{+} T_{reg}-gated populations also maintained that day 1 T_{regs} displayed a segregated clustering pattern based solely on $A_{2A}R$, PD-L1, CD39, and CD73; however, CD39 was not coexpressed with CD73 (*SI Appendix*, Fig. S5).

TGF-β contributes to T_{reg} development and acts as a T_{reg}-derived inhibitory cytokine (5). Although T_{regs} did not stain positive for surface TGF-β directly ex vivo (*SI Appendix*, Fig. S3*A*), day 7 T_{regs} significantly up-regulated both surface-displayed and intracellular TGF-β upon restimulation compared to nT_{reg}, day 1 T_{reg} (Fig. 4*D*), T_{conv}, and CTL subsets across all time points (*SI Appendix*, Fig. S3*B*). This is in direct contrast to the data generated by RNA-Seq where a transcriptional difference was not detected in the kinetics of TGF-β1/2/3
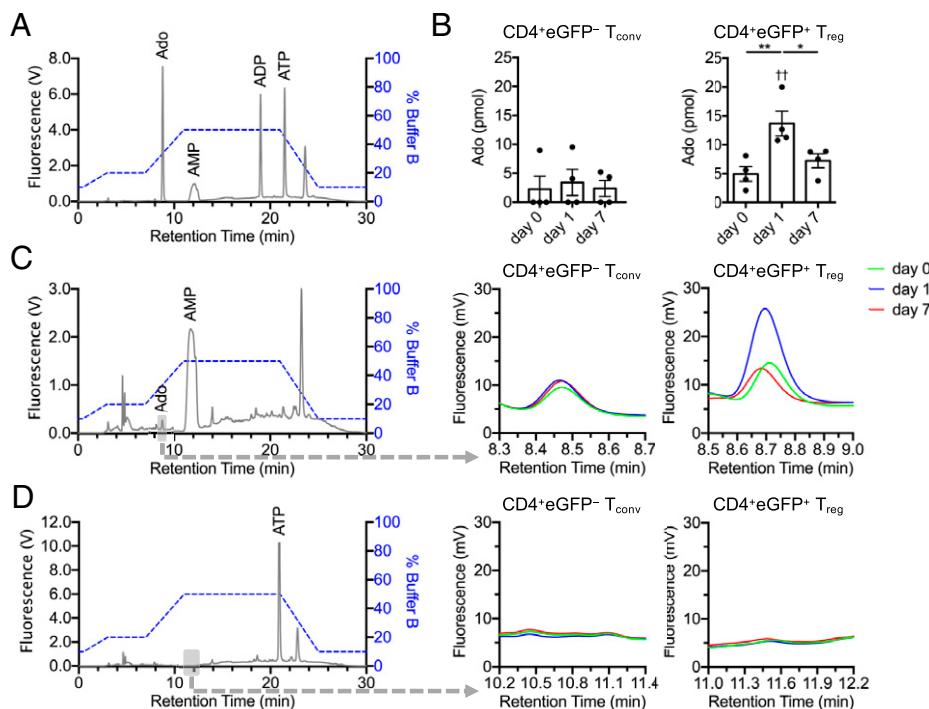
Dolina et al.
Developmentally distinct CD4^{+} T_{reg} lineages shape the CD8^{+}
T cell response to acute *Listeria* infection

Fig. 5. T_{regs} display increased CD73 enzymatic activity at day 1 postinfection. (*A*) A total of 10 pmol mixed 1,N^6-etheno-derivatized nucleotide standards (Ado, 5′-AMP, 5′-ADP, and 5′-ATP) resolved by HPLC. (*B–D*) FoxP3-eGFP$^+$ T_{regs} or FoxP3-eGFP$^-$ T_{convs} sorted from naïve (day 0) and *L. monocytogenes* Δ*actA*-Ova–infected (days 1 and 7) *Foxp3^{eGFP}* mice were placed in the upper chamber of a 96-well transwell plate. The bottom chamber was pulsed with either 10 μM 5′-AMP or 5′-ATP. (*B* and *C*) Concentration of Ado in the bottom chamber determined in cultures exposed to a 15-min 5′-AMP pulse for assessment of CD73 enzymatic activity, and (*D*) 5′-AMP similarly measured with a 15-min 5′-ATP pulse for measurement of CD39-mediated hydrolysis (*n* = 4 per group). Expanded retention times (gray box) for (*C*) Ado and (*D*) 5′-AMP are indicated. Mean ± SEM. (*B*) *P < 0.05 and **P < 0.01 (Student's *t* test); ††P < 0.01 (one-way ANOVA).

production across day 1 and day 7 T_{reg} populations (Fig. 3*D*). RNA-Seq analysis also suggested that a dominant feature in the late rising day 7 T_{regs} included increased adenylyl cyclases 3/7/9 and reduced phosphodiesterase 4 expression (Fig. 3*D*), which we hypothesized would positively correlate with intracellular cAMP. Consistent with this, we observed a gradual increase in T_{reg} cytosolic cAMP throughout the course of infection, with an increase in cAMP reaching significance by day 7 (Fig. 4*E*). Taken together, these data suggest that day 1 T_{regs} significantly up-regulate CD73 expression compared to nT_{regs}, and day 7 T_{regs} preferentially increase TGF-β production and accumulate intracellular cAMP.

CD73 Enzymatic Conversion of 5′-AMP to Adenosine Is Dominant in the Early Phase. CD73 expression on the cell surface does not strictly correlate with catabolic activity but is also synchronized with T_{reg} TCR engagement (27). CD73 is a C-terminal glycosyl-phosphatidylinositol (GPI) anchored protein that exists in dimeric soluble and membrane-bound forms. When expressed on the cell surface, CD73 switches between open/closed conformations where the open form is receptive to catalysis and has at least two distinct states (ranging from 977 to 1,609 Å) when actively bound to Ado due to a fluid homodimerization interface. Further, 5′-ATP and 5′-ADP are known to be natural competitive inhibitors of CD73 (28, 29). This suggests that its activity is also influenced by the microenvironment and associated cell damage occurring early during infection.

We therefore sought to determine whether there was a functional impact from the small increase in CD73 we observed in day 1 T_{regs}. Ado, 5′-AMP, 5′-ADP, and 5′-ATP can be converted into 1,N^6-etheno-derivatized nucleotide analogs, which can be resolved by high-performance liquid chromatography (HPLC)

and detected by fluorescence at 410 nm (Fig. 5*A*). To measure CD73 enzymatic activity, CD4$^+$FoxP3-eGFP$^-$ T_{convs} and CD4$^+$FoxP3-eGFP$^+$ T_{regs} were sorted from naïve and day 1 or day 7 infected *Foxp3^{eGFP}* mice. Cells were seeded in transwells under serum-free conditions, and 10 μM 5′-AMP or 5′-ATP substrates were pulsed in the opposing chamber of each well (free of cells) to test for CD73-mediated 5′-AMP to Ado and CD39-mediated 5′-ATP to 5′-AMP hydrolysis, respectively. Chambers devoid of cells were mixed and aliquoted after 15 min of incubation, derivatized, and assessed via HPLC. Our analysis confirmed that, in association with a subtle increase in CD73 surface expression, day 1 T_{regs} had greater than twofold increased enzymatic activity in converting 5′-AMP to Ado compared to nT_{regs} and day 7 T_{regs}. T_{convs} did not display any CD73 activity (Fig. 5 *B* and *C*). We also could not detect any CD39 activity by this method in T_{conv} or T_{reg} subsets (Fig. 5*D*). These findings support that day 1 T_{regs} are functionally hyperreactive to extracellular 5′-AMP during *L. monocytogenes* infection and can rapidly generate significant amounts of immunosuppressive Ado via CD73.

cAMP and TGF-β Separately Regulate Priming and Contraction Phases of the CD8$^+$ T Cell Response. Given the possible relevance of differential TGF-β, CD73-released Ado, and cAMP production/accumulation, we investigated the contextual relevance of these suppressive mediators during bimodal T_{reg} kinetics. We therefore evaluated the effect of blocking versus agonizing these pathways during in vitro CD3/CD28-based suppressor assays. TGF-β neutralization contributed equally to both day 1 and day 7 T_{regs} in vitro suppressor activity (*SI Appendix*, Fig. S4*A*), despite the fact that production and surface display of TGF-β was elevated by day 7 T_{regs} directly ex vivo compared to

Dolina et al.
Developmentally distinct CD4$^+$ T_{reg} lineages shape the CD8$^+$
T cell response to acute *Listeria* infection

PNAS | 7 of 12
https://doi.org/10.1073/pnas.2113329119

day 1 T_{regs} (Fig. 4D). We also noted that inclusion of anti–TGF-β in wells containing only CD8+ T_{resps} promoted additional proliferation over baseline responses to anti-CD3/CD28 agonism (*SI Appendix*, Fig. S4B), indicating that in vitro blockade of TGF-β may not accurately mirror T_{reg} production and surface display in vivo due to autocrine production of TGF-β by CD8+ T cells after acute and chronic TCR ligation seen in this report (*SI Appendix*, Fig. S3B) and others (30, 31).

Ado binding to $A_{2A}R$ on CD8+ T cells activates adenylyl cyclases, which in turn induces the synthesis of intracellular cAMP—which is ultimately inhibitory to the activity of these cells (23). cAMP directly binds PKA in a 4:1 stoichiometry leading to separation of PKA catalytic and regulatory subunits, whereupon the catalytic subunits of PKA activate C-terminal Src kinase (CSK) via phosphorylation of Ser364. pCSK in turn phosphorylates lymphocyte-specific protein tyrosine kinase (Lck) at Tyr505 to directly inhibit TCR signaling in T cells (32). Indirect suppression of CD8+ T_{resps} by T_{reg} CD73-derived Ado was therefore explored in this context. For this, CD4+FoxP3-eGFP+ T_{regs} sorted from naïve, day 1 infected, and day 7 infected $Foxp3^{eGFP}$ mice were placed in the upper chamber of transwell plates, above wells containing CD8+ T_{resps}. After CD3/CD28 stimulation of both subsets, CD8+ T_{resp} division was assessed. All T_{reg} suppressor activity, including any mechanism related to TGF-β provision or surface display, was contact dependent at every time point in the absence of CD73 5′-AMP substrate. After addition of 5′-AMP, only day 1 T_{regs} displayed suppressor activity in the absence of cell contact (Fig. 6A). This phenotype was consistently apparent in day 1 T_{reg}:T_{resp} cocultures with cell contact permitted (Fig. 6B). Importantly, $Adora2a^{-/-}$ CD8+ T_{resp} (lacking $A_{2A}R$) division was not impeded after addition of 5′-AMP compared to isogenic BALB/c CD8+ T_{resps} when cocultured with day 1 T_{regs} (Fig. 6C). We also compared the timing of suppression in vitro to an in vivo CD73 antibody blockade approach. In vivo reduction in the magnitude of the day 7 peak Ova-specific CD8+ T cell response against *L. monocytogenes* $\Delta actA$-Ova was apparent after early (days 0 to 2) but not late (days 5 to 6) blockade of CD73. The in vivo effect of anti-CD73–mediated inhibition of CTL responses was entirely dependent on the presence of T_{regs}, as depletion of T_{regs} by administration of diphtheria toxin (DT) to $Foxp3^{DTR-eGFP}$ mice negated this effect (Fig. 6D).

Cytoplasmic cAMP can be directly transferred from T_{regs} to T_{resps} via gap junction intercellular communication (GJIC) (33). Despite inhibiting TCR signaling in T_{convs} and CTLs, cAMP does not inhibit TCR signals in T_{regs}, but rather enhances FoxP3 expression (34). As day 7 T_{regs} significantly accumulated intracellular cAMP compared to nT_{regs} and day 1 T_{regs} (Fig. 4E), we determined whether this was critical for cell contact–dependent suppression. CD4+FoxP3-eGFP+ T_{regs} were sorted from naïve, day 1 infected, and day 7 infected $Foxp3^{eGFP}$ mice and placed in coculture with CD8+ T_{resps} in the presence of $Gap27_{204–214}$ connexin mimetic peptide, known to interfere with gap junction formation and stability (33). As before, nT_{regs} and day 1 T_{regs} displayed ~50 to 60% suppression, and day 7 T_{regs} displayed ~80% suppression in the presence of a sequence-scrambled control peptide. Blockade of GJIC with $Gap27_{204–214}$ was sufficient to significantly reduce day 7 T_{reg} suppression by ~40 to 50%; however, GJIC blockade did not impact suppression mediated by nT_{regs} or day 1 T_{regs} (Fig. 6E). GJIC blockade also led to an increased concentration of IL-2 in the supernatants of day 7 T_{reg}:T_{resp} cocultures (Fig. 6F). $Gap27_{204–214}$ inhibited phosphorylation of cAMP-responsive element binding protein (CREB) in T_{resps}, suggesting that cAMP was included among the contents transferred via GJIC (Fig. 6G, *Upper*). Lastly, addition of a PKA inhibitor (KT5720) completely accounted for GJIC-mediated pCREB and $Gap27_{204–214}$ reversal of suppression in day 7 T_{reg}:T_{resp}

cocultures (Fig. 6 G and H). In vitro evidence therefore supported that day 1 T_{regs} provide abundant Ado in the surrounding extracellular microenvironment in regulating the priming of CTLs early after *L. monocytogenes* infection via a cell contact–independent mechanism. In contrast, day 7 T_{regs} are entirely dependent on cell contact–dependent suppression during the contraction phase of the CTL response and rely on cAMP GJIC transfer mechanisms (and likely elevated TGF-β production).

We questioned whether the timing of the distinct in vitro suppressor pathways translated to *L. monocytogenes* infection in vivo. Because GJIC cannot be blocked in vivo, we focused on evaluating the impact of single or dual TGF-β and CD73 antibody–mediated blockade administered early (days 0 to 2) or late (days 5 to 6) after infection. Splenic Ova-specific CD8+ T cell number was assessed by tetramer staining at day 7 postinfection. We found that early anti-CD73 boosted the number of Ova-specific CD8+ T cells. In contrast, anti–TGF-β led to increased antigen-specific CTL numbers at later time points. A combination of anti–TGF-β and anti-CD73 did not reveal any additive or synergistic effects (Fig. 7A). With DT-mediated depletion of T_{regs} in infected $Foxp3^{DTR-eGFP}$ mice, delayed TGF-β blockade alone or in combination with anti-CD73 did not impact Ova-specific CD8+ T cell frequency or absolute number (Fig. 7B). Therefore, the role of CD73 in T_{reg} suppressor function was consistent with an early cell contact–independent mechanism on CD8+ T cells, whereas late inhibition of CTL responses by T_{regs} aligned with cell contact–dependent mechanisms in part involving TGF-β surface display and cAMP transfer. These data collectively support that distinct T_{reg} populations and suppressor mechanisms arise to separately control priming and contraction phases of the CTL response during a single acute infection (Fig. 7C).

Discussion

A wealth of studies has led to the view that T_{reg} responses in infection, cancer, and autoimmunity are essentially monophasic (i.e., similar in terms of suppressor cells and molecular mechanisms). Here we demonstrate that T_{regs} display a sequential, biphasic expansion pattern in response to an infectious pathogen that is composed of developmentally distinct suppressor cell populations, which separately control the CD8+ T cell response during priming versus contraction stages. Following *L. monocytogenes* infection, day 1 T_{regs} arise in response to elevated microbial presence, activate a CD73-mediated suppressor mechanism, and rapidly produce Ado in order to fine-tune CD8+ T cell priming via cell contact–independent suppression. This first wave of regulation is transient, however, as the number of T_{regs} markedly decreases by day 3, as does their suppressive capacity per cell, commensurate with the primary expansion of pathogen-specific CD8+ T cells. When *L. monocytogenes* antigen is cleared and CD8+ T cell accumulation reaches its day 7 peak, a distinct population of T_{regs} appears that relies primarily on cell contact–dependent transfer of cAMP to initiate and/or in part support T cell contraction. These findings reveal an unexpected plasticity in the T_{reg} response to acute infection, which employs distinct populations, expansion kinetics, and effector mechanisms early after pathogen sensing to avoid inflammation-induced immunopathology by CD8+ T cells versus late in the response to restore homeostasis. Importantly, our data show that early T_{reg}-mediated suppression is short lived, presumably to avoid impeding the expansion of pathogen-specific CD8+ T cells that are needed for host defense once they have exerted an initial role in protecting the host from autoimmune- or inflammation-mediated pathology caused by systemic activation. Taken together, our findings reveal that, rather than being a unitary monophasic
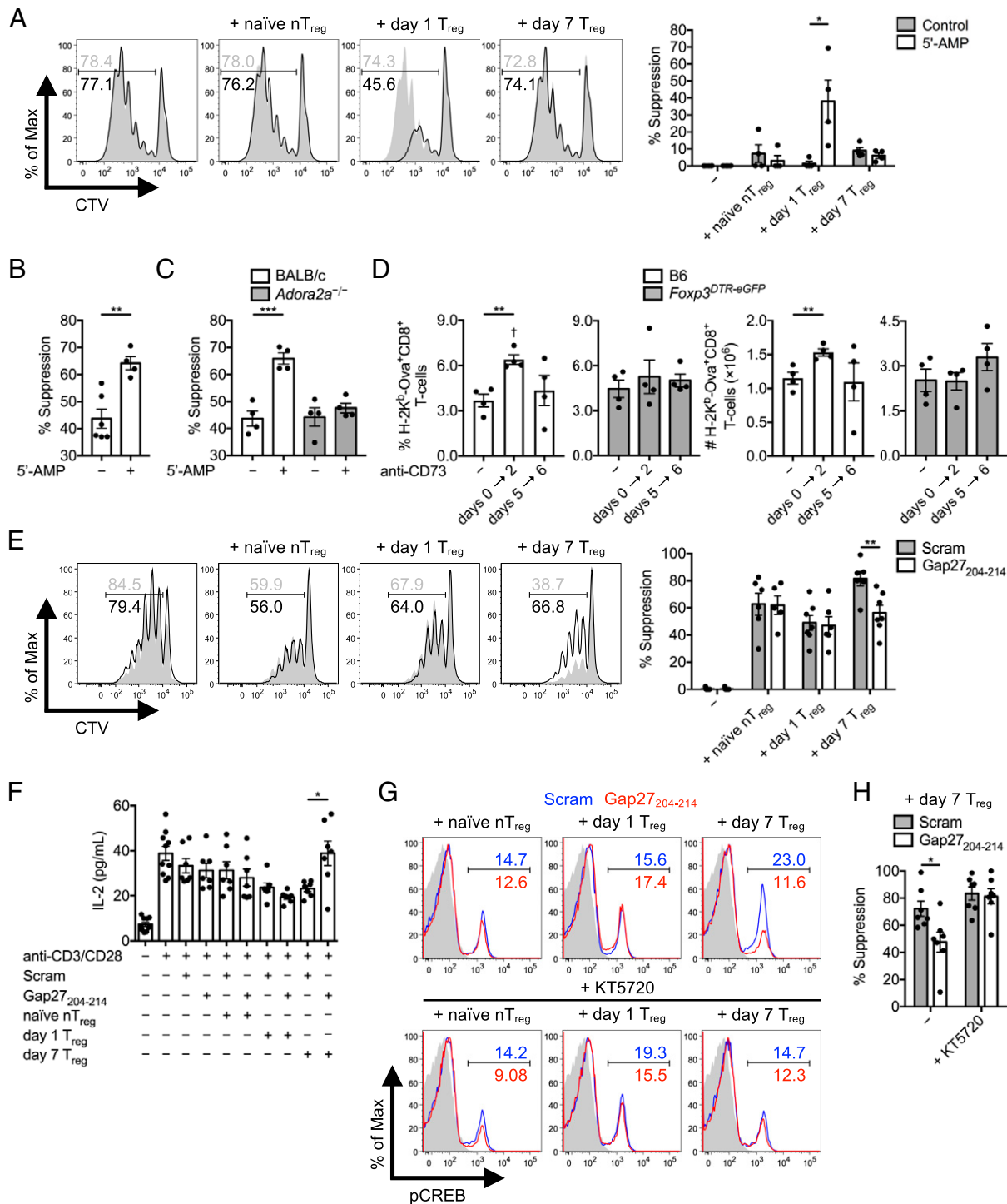
Dolina et al.
Developmentally distinct CD4+ T_{reg} lineages shape the CD8+
T cell response to acute *Listeria* infection

Fig. 6. Day 1 versus day 7 bimodal T_{reg} cAMP-mediated suppression. (*A*) CD45.2$^+$CD4$^+$FoxP3-eGFP$^+$ T_{regs} sorted from naïve and day 1 or day 7 *L. monocytogenes* Δ*actA*-Ova–infected *Foxp3^{eGFP}* mice were placed in the upper chamber of a 96-well transwell plate, with the bottom chamber containing naïve CTV-labeled CD45.1$^+$CD8$^+$ T_{resps}. At day 3 after anti-CD3/CD28 stimulation, CD45.1$^+$CD8$^+$ T_{resp} percent suppression in the presence or absence of 1 μM 5′-AMP was assessed (*n* = 4 per group). In vitro CD45.2$^+$CD8$^+$ T_{resp} proliferation of (*B*) C57BL/6 or (*C*) BALB/c compared to *Adora2a$^{-/-}$* origin represented as percent suppression at day 3 after a cell-contact permissive, 1:1 coculture of naïve CTV-labeled CD45.2$^+$CD8$^+$ T_{resps} with CD45.1$^+$CD4$^+$FoxP3-eGFP$^+$ T_{regs} isolated from day 1 infected CD45.1$^+$ *Foxp3^{eGFP}* mice in the presence or absence of 1 μM 5′-AMP (*n* = 4 per group). (*D*) The percent and absolute number of splenic Ova-specific CD8$^+$ T cells at day 7 postinfection of C57BL/6 and *Foxp3$^{DTR-eGFP}$* mice infected with *L. monocytogenes* Δ*actA*-Ova. DT injection dictated T_{reg} depletion with control and early (days 0 to 2) versus late (days 5 to 6) CD73 blockade compared (*n* = 4 per group). (*E*) In vitro CD45.1$^+$CD8$^+$ T_{resp} percent suppression and (*F*) IL-2 detected in supernatant at day 3 after 1:1 coculture with CD45.2$^+$CD4$^+$FoxP3-eGFP$^+$ T_{regs} isolated from naïve and day 1 or day 7 infected CD45.1$^+$ *Foxp3^{eGFP}* mice in the presence or absence of Gap27$_{204-214}$ or scrambled control peptide (*n* = 6 to 10 per group). (*G* and *H*) Suppressor assay as in *E* and *F* with KT5720 selective inhibition of PKA with analysis of intracellular pCREB in CD45.1$^+$CD8$^+$ T_{resps}, and percent suppression exerted by day 7 T_{regs} (*n* = 7 per group). Numbers in histograms represent percentage. Mean ± SEM. (*A–F* and *H*) *$P < 0.05$, **$P < 0.01$, and ***$P < 0.001$ (Student's *t* test); (*D*) †$P < 0.05$ (one-way ANOVA relative to negative control).
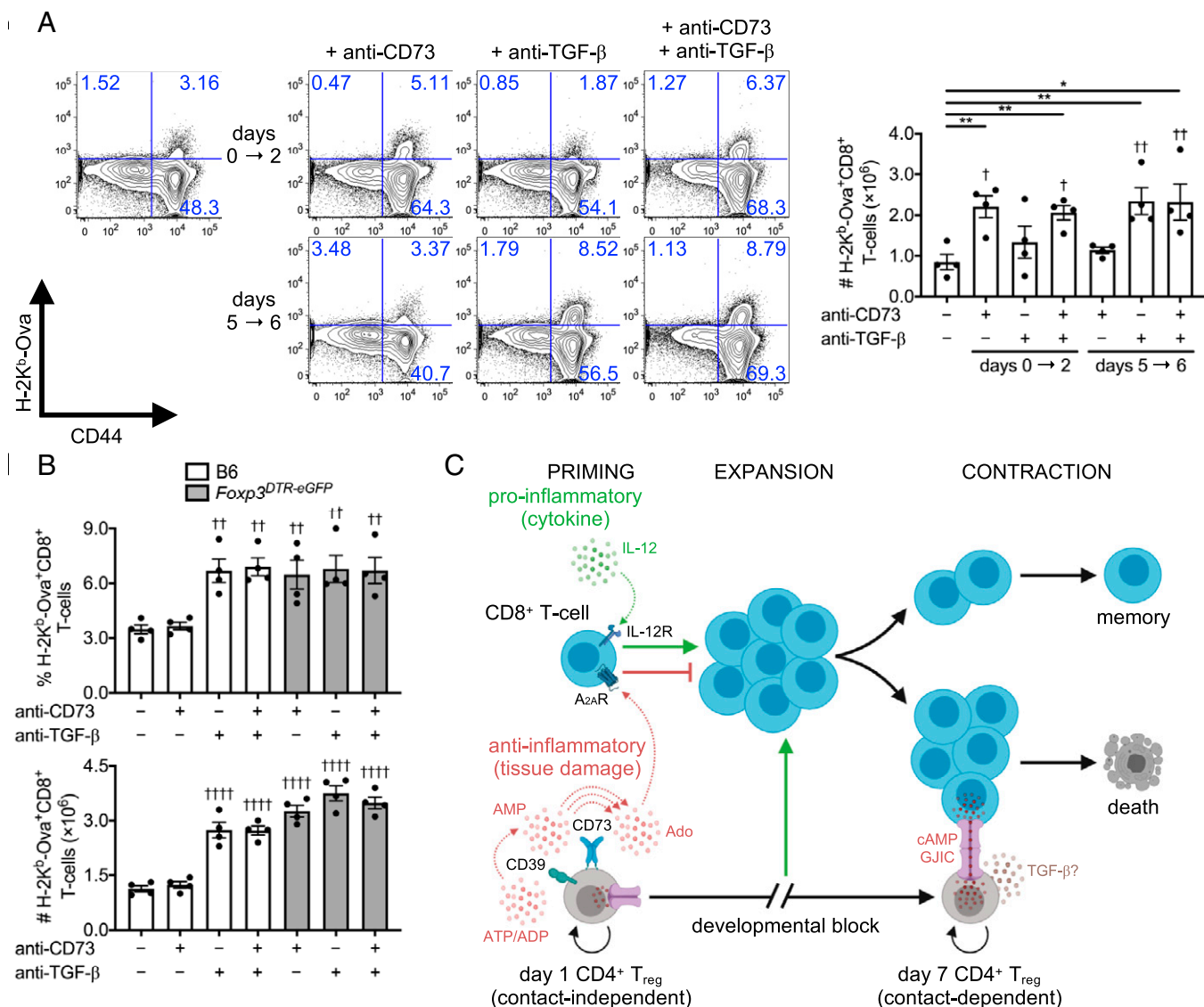
Dolina et al.
Developmentally distinct CD4$^+$ T_{reg} lineages shape the CD8$^+$
T cell response to acute *Listeria* infection

PNAS | 9 of 12
https://doi.org/10.1073/pnas.2113329119

IMMUNOLOGY AND
INFLAMMATION

Fig. 7. The CD73 pathway suppresses Ova-specific CD8$^+$ T cell responses early after *Listeria* infection in vivo. (*A*) C57BL/6 mice infected with *L. monocytogenes* Δ*actA*-Ova. Absolute number of Ova-specific CD8$^+$ T cells at 7 d postinfection in spleens with control and early (days 0 to 2) versus late (days 5 to 6) TGF-β and CD73 single and dual blockade compared ($n = 4$ per group). (*B*) Percent and absolute number of splenic Ova-specific CD8$^+$ T cells at day 7 after *L. monocytogenes* Δ*actA*-Ova infection of C57BL/6 versus *Foxp3$^{DTR-eGFP}$* mice. DT injection dictated specific T$_{reg}$ depletion with control and late (days 5 to 6) TGF-β and CD73 single and dual blockade compared ($n = 4$ per group). (*C*) Proposed model for biphasic T$_{reg}$ response to *L. monocytogenes* infection. Numbers in scatterplots represent percentage. Mean ± SEM. (*A*) *$P < 0.05$ and **$P < 0.01$ (Student's *t* test); (*A* and *B*) †$P < 0.05$, ††$P < 0.01$, and ††††$P < 0.0001$ (one-way ANOVA relative to negative control).

force opposing the induction of immunity, T$_{reg}$-mediated regulation is more dynamic, varied, and coordinated than has been previously described.

Regarding the ontogeny of the early (day 1) versus late (day 7) T$_{reg}$ populations, we found no evidence of a developmental relationship using both lineage tracing (BrdU and EdU copulsing) and genetic (TCR-Seq) approaches, suggesting that these subpopulations arise from distinct progenitors. In previous work from our laboratory using the *L. monocytogenes* model, it was found that the day 1 T$_{reg}$ population is a mixture of activated nT$_{regs}$ and T$_{convs}$ that rapidly up-regulate FoxP3 and accumulate in the secondary lymphoid tissues of infected animals (20). The present work extends these findings through identification of the second day 7 T$_{reg}$ population that appears clonally distinct from day 1 T$_{regs}$ and shows only ~0.5 to 1.5% overlap in TCR clonotypes with T$_{convs}$ (Fig. 2*E*). We therefore

hypothesize that the majority of day 7 T$_{regs}$ are newly emergent nT$_{regs}$ that replace the original nT$_{reg}$ population present during homeostasis and early after infection (days 0 to 1). From a kinetic standpoint, it is also unlikely that day 1 T$_{regs}$ are antigen-specific, whereas day 7 T$_{regs}$ presumably contain a small fraction of clonotypes specific to *L. monocytogenes*.

The presence and suppressive capacity of day 1 T$_{regs}$ are instead linked to the amount of inflammation, and not antigen, associated with increased initial *L. monocytogenes* exposure (20). More specifically, early neutrophil release of self-DNA as part of neutrophil extracellular trap (NET) generation has been suggested as a means by which tissue damage can be sensed in this model, enabling day 1 T$_{regs}$ to fine-tune CTL responses to avoid immunopathology (20, 35, 36). We hypothesize that the generation of day 1 T$_{regs}$ is a two-step process. In the first step, inflammatory cytokines and NET-derived self-

Dolina et al.
Developmentally distinct CD4$^+$ T$_{reg}$ lineages shape the CD8$^+$
T cell response to acute *Listeria* infection

DNA serve as initiating signals for T_{conv} to T_{reg} conversion. In the second step, damage-associated adenine nucleotides are used as mediators of suppression. We have previously shown that, in the context of acute *L. monocytogenes* exposure, DNA released by neutrophils directly engages Toll-like receptor 9 (TLR9) on CD8α+ dendritic cells, which in turn is necessary and sufficient to support early day 1 T_{reg} differentiation and accumulation (20). This occurs rapidly (in less than 6 h) and precedes the onset of tissue damage evidenced by later systemic rises in serum aspartate aminotransferase and alanine aminotransferase (AST/ALT) peaking at 2 d postinfection (20, 37). In this study, we can extend this mechanism by demonstrating that the rapidly generated T_{regs} utilize adenine nucleotides released from damaged tissues into the early phase of this immunoregulatory circuit. CD73 exerts early immunosuppression on CTL responses only in the presence of an intact T_{reg} population. Day 1 T_{regs} express elevated levels of functional CD73 and suppress CD8+ T_{resps} in the absence of cell contact. We speculate that, as tissue damage leads to adenine nucleotide release, day 1 CD73+ T_{regs} respond by enzymatically increasing extracellular Ado concentration gradients. Once present in the extracellular milieu, Ado is poised to directly engage $A_{2A}R$ on CD8+ T cells in the local microenvironment to directly inhibit activation (23). Ado-mediated suppression early after infection may therefore endow day 1 T_{regs} with the ability to effectively monitor tissue damage and exert control on the amount of potentially autoreactive CD8+ T cells generated at priming.

Immunosuppression by T_{reg} occurs through both cell contact–dependent and –independent mechanisms (1, 13, 38). Accordingly, we found both types operative within the regulatory circuit we describe. Whereas day 7 T_{regs} solely relied on cell contact–dependent mechanisms, including cAMP transfer via GJIC, day 1 T_{reg} suppression was conversely mediated by a CD73 cell contact–independent mechanism. We propose that early cell contact–independent mechanisms are rapidly implemented to quickly counteract tissue damage when detected. These T_{regs} can be rapidly deployed to limit the activation of resident and/or nonresident memory T cells, known to be activated by bystander proinflammatory cytokines in the absence of antigen (39–41). We further speculate that cAMP transfer events act as part of a late phase restoration of homeostasis compared to the early burst of T_{reg} Ado. Lastly, the kinetics of day 1 and day 7 T_{reg} suppressor populations appear to be elegantly choreographed to accommodate the dynamics of the natural pathogen-specific CD8+ T cell response, with an early day 1 response that can protect the acutely infected host from immunopathology, a subsequent lull in T_{reg} activity to permit the expansion of pathogen-specific CD8+ T cells, and a late day 7 phase of regulation to assist in the restoration of homeostasis (Fig. 7C). Of note, the in vitro suppression assay utilized herein only accounts for T_{reg}:T_{resp} communication and does not account for the role of APCs, emphasizing the need for further research into the role of this latter population in light of its critical position in integrating innate signals during CD8+ T cell priming. Nevertheless, this report reveals insights into how T_{regs} function as a dynamic "rheostat" in adaptive immunity that is able to amplify versus inhibit CD8+ effector T cell responses at a time and in a manner that is most beneficial to the host.

In summary, this study shows that T_{reg} immunosuppression of CD8+ T cells directed against an acute infection is dynamic and orchestrated with distinct phases that follow the rise and fall of the adaptive immune response. Importantly, these data define the discrete temporal and functional windows in which T_{regs} operate and give insights into the distinct effector mechanism(s) used in each. Rapid T_{reg} plasticity is likely a common feature controlling cell-mediated immunity and is necessary to tightly resolve pathogenic threats while efficiently balancing self-reactivity. A closer examination and deeper analysis of this bimodal response may open up new research areas for understanding the complexities of T_{reg} development, TCR specificity to self- versus foreign-antigen and overall relevance to immunosuppression, and the cues that dictate T_{reg} function and presence. These findings may also aid in vaccination strategies to optimize the balance between CD8+ T cell priming and ultimate formation of memory.

Materials and Methods

Standard procedures for CD4+ and CD8+ T cell isolation and coculture, *L. monocytogenes* infection, hemisplenectomy, antibody/peptide/small molecule treatments, HPLC, enzyme-linked immunosorbent assay (ELISA), and fluorescence-activated cell sorting (FACS), as well as detailed descriptions of RNA-Seq/TCR-Seq experiments and data analysis are described in *SI Appendix, SI Materials and Methods*. Animals were used according to protocols approved by the La Jolla Institute for Immunology.

1. S. Sakaguchi, K. Wing, Y. Onishi, P. Prieto-Martin, T. Yamaguchi, Regulatory T cells: How do they suppress immune responses? *Int. Immunol.* **21**, 1105–1111 (2009).
2. S. Sakaguchi, D. A. A. Vignali, A. Y. Rudensky, R. E. Niec, H. Waldmann, The plasticity and stability of regulatory T cells. *Nat. Rev. Immunol.* **13**, 461–467 (2013).
3. J. B. Wing, S. Sakaguchi, TCR diversity and Treg cells, sometimes more is more. *Eur. J. Immunol.* **41**, 3097–3100 (2011).
4. S. Sakaguchi, N. Sakaguchi, M. Asano, M. Itoh, M. Toda, Immunologic self-tolerance maintained by activated T cells expressing IL-2 receptor alpha-chains (CD25). Breakdown of a single mechanism of self-tolerance causes various autoimmune diseases. *J. Immunol.* **155**, 1151–1164 (1995).
5. C. Benoist, D. Mathis, Treg cells, life history, and diversity. *Cold Spring Harb. Perspect. Biol.* **4**, a007021–a007021 (2012).
6. E. M. Dons, G. Raimondi, D. K. C. Cooper, A. W. Thomson, Induced regulatory T cells: Mechanisms of conversion and suppressive potential. *Hum. Immunol.* **73**, 328–334 (2012).
7. J. D. Fontenot et al., Regulatory T cell lineage specification by the forkhead transcription factor foxp3. *Immunity* **22**, 329–341 (2005).
8. S. F. Ziegler, FOXP3: Of mice and men. *Annu. Rev. Immunol.* **24**, 209–226 (2006).
9. K. Kretschmer et al., Inducing and expanding regulatory T cell populations by foreign antigen. *Nat. Immunol.* **6**, 1219–1227 (2005).
10. M. Yadav, S. Stephan, J. A. Bluestone, Peripherally induced tregs—Role in immune homeostasis and autoimmunity. *Front. Immunol.* **4**, 232 (2013).
11. S. Z. Josefowicz, L.-F. Lu, A. Y. Rudensky, Regulatory T cells: Mechanisms of differentiation and function. *Annu. Rev. Immunol.* **30**, 531–564 (2012).
12. Y. Togashi, K. Shitara, H. Nishikawa, Regulatory T cells in cancer immunosuppression—Implications for anticancer therapy. *Nat. Rev. Clin. Oncol.* **16**, 356–371 (2019).
13. Y. Belkaid, K. Tarbell, Regulatory T cells in the control of host-microorganism interactions (*). *Annu. Rev. Immunol.* **27**, 551–589 (2009).
14. A. Benson et al., Microbial infection-induced expansion of effector T cells overcomes the suppressive effects of regulatory T cells via an IL-2 deprivation mechanism. *J. Immunol.* **188**, 800–810 (2012).
15. T. Chinen et al., An essential role for the IL-2 receptor in T_{reg} cell function. *Nat. Immunol.* **17**, 1322–1333 (2016).
16. Y. Belkaid, B. T. Rouse, Natural regulatory T cells in infectious disease. *Nat. Immunol.* **6**, 353–360 (2005).
17. R. Cabrera et al., An immunomodulatory role for CD4(+)CD25(+) regulatory T lymphocytes in hepatitis C virus infection. *Hepatology* **40**, 1062–1071 (2004).
18. J. H. Rowe, J. M. Ertelt, M. N. Aguilera, M. A. Farrar, S. S. Way, Foxp3(+) regulatory T cell expansion required for sustaining pregnancy compromises host defense against prenatal bacterial pathogens. *Cell Host Microbe* **10**, 54–64 (2011).
19. B. J. Laidlaw et al., Production of IL-10 by CD4(+) regulatory T cells during the resolution of infection promotes the maturation of memory CD8(+) T cells. *Nat. Immunol.* **16**, 871–879 (2015).
20. J. S. Dolina et al., TLR9 sensing of self-DNA controls cell-mediated immunity to Listeria infection via rapid conversion of conventional CD4+ T cells to T_{reg}. *Cell Rep.* **31**, 107249 (2020).

Dolina et al.
Developmentally distinct CD4+ T_{reg} lineages shape the CD8+ T cell response to acute *Listeria* infection

PNAS | 11 of 12
https://doi.org/10.1073/pnas.2113329119

IMMUNOLOGY AND INFLAMMATION

21. J. M. Ertelt *et al.*, Foxp3+ regulatory T cells impede the priming of protective CD8+ T cells. *J. Immunol.* **187**, 2569–2577 (2011).

22. J. M. Kim, J. P. Rasmussen, A. Y. Rudensky, Regulatory T cells prevent catastrophic autoimmunity throughout the lifespan of mice. *Nat. Immunol.* **8**, 191–197 (2007).

23. M. Klein, T. Bopp, Cyclic AMP represents a crucial component of Treg cell-mediated immune regulation. *Front. Immunol.* **7**, 315 (2016).

24. D. Peter, S. L. C. Jin, M. Conti, A. Hatzelmann, C. Zitt, Differential expression and function of phosphodiesterase 4 (PDE4) subtypes in human primary CD4+ T cells: Predominant role of PDE4D. *J. Immunol.* **178**, 4820–4831 (2007).

25. N. Safinia, C. Scotta, T. Vaikunthanathan, R. I. Lechler, G. Lombardi, Regulatory T cells: Serious contenders in the promise for immunological tolerance in transplantation. *Front. Immunol.* **6**, 438 (2015).

26. Y. Kitazawa *et al.*, Involvement of the programmed death-1/programmed death-1 ligand pathway in CD4+CD25+ regulatory T-cell activity to suppress alloimmune responses. *Transplantation* **83**, 774–782 (2007).

27. L. Antonioli, P. Pacher, E. S. Vizi, G. Haskó, CD39 and CD73 in immunity and inflammation. *Trends Mol. Med.* **19**, 355–367 (2013).

28. B. Allard, M. S. Longhi, S. C. Robson, J. Stagg, The ectonucleotidases CD39 and CD73: Novel checkpoint inhibitor targets. *Immunol. Rev.* **276**, 121–144 (2017).

29. K. Knapp *et al.*, Crystal structure of the human ecto-5′-nucleotidase (CD73): Insights into the regulation of purinergic signaling. *Structure* **20**, 2161–2173 (2012).

30. M. O. Li, Y. Y. Wan, S. Sanjabi, A.-K. L. Robertson, R. A. Flavell, Transforming growth factor-beta regulation of immune responses. *Annu. Rev. Immunol.* **24**, 99–146 (2006).

31. R. Tinoco, V. Alcalde, Y. Yang, K. Sauer, E. I. Zuniga, Cell-intrinsic transforming growth factor-beta signaling mediates virus-specific CD8+ T cell deletion and viral persistence in vivo. *Immunity* **31**, 145–157 (2009).

32. V. L. Wehbi, K. Taskén, Molecular mechanisms for cAMP-mediated immunoregulation in T cells—Role of anchored protein kinase A signaling units. *Front. Immunol.* **7**, 222 (2016).

33. T. Bopp *et al.*, Cyclic adenosine monophosphate is a key component of regulatory T cell-mediated suppression. *J. Exp. Med.* **204**, 1303–1310 (2007).

34. A. Y. Wen, K. M. Sakamoto, L. S. Miller, The role of the transcription factor CREB in immune function. *J. Immunol.* **185**, 6413–6419 (2010).

35. S.-T. Chen *et al.*, CLEC5A is a critical receptor in innate immunity against Listeria infection. *Nat. Commun.* **8**, 299 (2017).

36. A. R. Witter, B. M. Okunnu, R. E. Berg, The essential role of neutrophils during infection with the intracellular bacterial pathogen Listeria monocytogenes. *J. Immunol.* **197**, 1557–1565 (2016).

37. T. Miura *et al.*, Roles of endogenous cytokines in liver apoptosis of mice in lethal Listeria monocytogenes infection. *FEMS Immunol. Med. Microbiol.* **28**, 335–341 (2000).

38. K. H. G. Mills, Regulatory T cells: Friend or foe in immunity to infection? *Nat. Rev. Immunol.* **4**, 841–855 (2004).

39. D. Herndler-Brandstetter *et al.*, KLRG1^{+} effector CD8^{+} T cells lose KLRG1, differentiate into all memory T cell lineages, and convey enhanced protective immunity. *Immunity* **48**, 716–729.e8 (2018).

40. J. T. Ingram, J. S. Yi, A. J. Zajac, Exhausted CD8 T cells downregulate the IL-18 receptor and become unresponsive to inflammatory cytokines and bacterial co-infections. *PLoS Pathog.* **7**, e1002273 (2011).

41. D. F. Tough, P. Sun, X. Zhang, J. Sprent, Stimulation of memory T cells by cytokines. *Vaccine* **18**, 1642–1648 (2000).

42. J. S. Dolina *et al.*, Systemic inflammation drives rapid conversion of conventional CD4+ T cells to T_{reg} in vivo. NCBI Gene Expression Omnibus (GEO). https://www.ncbi.nlm.nih.gov/geo/query/acc.cgi?acc=GSE169741. Deposited 26 March 2021.

12 of 12 | **PNAS**
https://doi.org/10.1073/pnas.2113329119

Dolina et al.
Developmentally distinct CD4^{+} T_{reg} lineages shape the CD8^{+}
T cell response to acute *Listeria* infection